Chapter 2

Theoretical background

Contents

2.1 Introduction

This chapter presents a theoretical basis on which this research project will be grounded. Firstly a short description is given of light, as it is the only way information was gathered for this project.

To cover the subject of star formation, a broad approach is taken by describing the interstellar medium. Different phases are discussed where star formation occurs and where young stars are most

commonly found. A section is dedicated to star formation, describing the different phases and the initial mass function. A short section related to **p**re-**m**ain **s**equence (PMS) stars then describes the properties of young stars which actively collect matter from the molecular cloud from which they formed.

An entire section is dedicated to T Tauri stars, as the main objective of this project is to confirm whether there are T Tauri stars in the vicinity of RCW 34. The different classes of T Tauri stars are described as well as the type of emission seen in each type. A section then follows describing the types of grouping in which T Tauri stars are found. The chapter ends with short sections on photometry and spectroscopy.

2.2 Light - the information carrier of astronomy

2.2.1 Light and its interaction with the atmosphere

The only information that can be directly observed from stars is electromagnetic radiation. Electromagnetic radiation, or light, is found in quantised packets called photons. A photon's energy is directly proportional to the frequency of the light, given by

$$E = h\nu = h\frac{c}{\lambda} \ , \tag{2.1}$$

where $h = 6.62606 \times 10^{-34}$ J.s (Planck's constant), ν the frequency of the light, c the velocity of light in a vacuum and λ the wavelength of the photon. The wavelengths of photons emitted by different star types can range from the long wavelengths (10-100 m) of radio-waves, to very short wavelengths (<1-nm) of γ-rays. The Earth's atmosphere absorbs much of the incident light from stars so that only a fraction of the light is observable by ground instruments. The largest windows for ground based observations are for radio waves, infrared and optical light. For other parts of the spectrum, most of the light gets absorbed by molecules or it may get scattered by gas and dust in the atmosphere.

2.2.2 Stellar emission

A star emits radiation from its photosphere, which in a function of its surface temperature. If it is assumed that a star radiates like a black body, its electromagnetic emission profile can be expressed by the Planck spectrum

$$I(\nu, T) = \frac{2h\nu^3}{c^2}\frac{1}{e^{h\nu/kT} - 1} \ , \tag{2.2}$$

with $I(\nu, T)$ the mean photon intensity, ν the frequency, h Planck's constant, c the velocity of light, k Boltzmann's constant and T the temperature of the body. Assuing that the emission profile from a star is similar to that of a blackbody one can say that $I(\nu, T) = B(\nu, T)$, with $B(\nu, T)$ the black body spectrum; The average number of photons emitted by a black body with a temperature of T at a

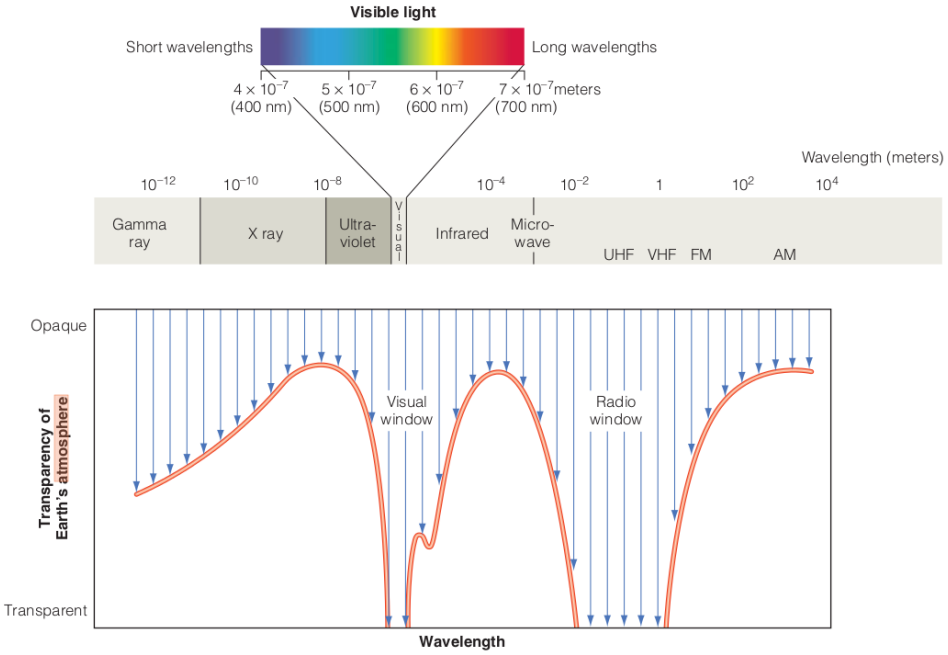

Figure 2.1: A reproduction of Fig 6.3 in Seeds (1997) showing which parts of the electromagnetic spectrum propagate through the atmosphere.

frequency of ν, can thus be given by dividing the intensity with the photon energy $h\nu$,

$$N(\nu, T) = \frac{2\nu^2}{c^2} \frac{1}{e^{h\nu/kT} - 1} \ . \tag{2.3}$$

Light emitted by stars spans a vast range in ν across the electromagnetic spectrum. The types of devices used to observe the light are limited to device-specific parts of the electromagnetic spectrum. This is because light in different parts of the spectrum interacts with a detector and with the atmosphere in different ways. For wavelengths longer than 1-mm a radio-antenna is used, between 1-mm to 1-μm an infrared array is used, between 1-μm to 0.4-μm an optical CCD is used; for 0.4-μm to 0.01-μm an ultraviolet CCD is used and from 0.01-μm to 1-nm an X-ray detector is used. This study was conducted in the optical part of the spectrum ranging from 4000 Å to 7000 Å.

The type of stars that are of concern to this study are very young and usually found in gaseous environments. Light emitted from these young stars not only interacts with particles in the earth's atmosphere, but also with the locally associated gaseous environments. A description of these localised gaseous environments follows.

2.3 The interstellar medium

The **i**nter**s**tellar **m**edium (ISM) is considered to be any matter that is found outside of a star's photosphere. The ISM consists of gas and dust particles, which is composed of 75% hydrogen, 25% helium and a small fraction of other elements and molecules.

The primordial ISM looked completely different to its current form. It was formed shortly after the Big Bang as a homogeneous isotropic distribution of protons, electrons and neutrons. The only elements that could be formed through nucleosynthesis in the warm radiation-dominated universe were Deuterium, Helium, Helium-3 and Helium-4. After the universe expanded significantly, the sea of Hydrogen neutralised and cooled. The first large-scale structures were formed during this period of abundant neutral hydrogen. These large-scale structures and the continuous expansion of the universe caused a further drastic change in the isotropic distribution of the hydrogen. Presently the ISM developed a clumpy distribution, ranging from dense molecular clouds to very low densities in locations devoid of any luminous object.

Today, the chemical composition of the ISM is also significantly different from its initial composition. The major components of the ISM are still composed of hydrogen and He, while heavier elements have been added by means of expulsion from stars by means of stellar winds, supernovae explosions and other ejection mechanisms. Elements heavier than lithium and lighter than iron are created in the interiors of stars through nuclear fusion. Elements lighter than iron release energy when they are formed through nuclear fusion, while elements heavier than iron require energy to form through fusion. Each generation of stars enriches the ISM with heavy elements. For more in-depth discussions on the evolution of the ISM see Pagel (1997), Longair (2008) and Kitchin (1987).

2.3.1 Molecular clouds

The majority of the molecular gas in galaxies such as the Milky Way is to be found in massive clouds. The typical molecular cloud is described by Tielens (2005) to have a size of 40 pc, a mass of $4{\times}10^4$ $M_\odot$, a density in the vicinity of 200 particles.cm^{-3} and a temperature in the range of 10-20 K. A molecular cloud is subject to change because it is exposed to many thermal mechanisms, for example internal heating, due to turbulence and cooling by emission. These thermal processes roughly balance each other out so that the system can be considered to be in thermal equilibrium. This implies that the cloud has a uniform pressure and can also be regarded as static. For a uniform gas with a density of ρ_0 and a temperature of T_0 to contract and collapse under its own mass and trigger star formation it has to exceed the **Jeans mass**

$$M_J = \frac{4\pi^{\frac{3}{2}}}{3}\left(\frac{\gamma RT}{G}\right)^{3/2}\rho_0^{-\frac{1}{2}} \approx 10^4 M_\odot T_{100}^{\frac{3}{2}} n_{10000}\ , \tag{2.4}$$

where $T_{100} = T_0/100$ with the assumption that $T_0 < 100$ K, $n_{10000} = n_0/10^4$ g/cm^3, $n_0 \approx \rho_0/m_p$ and $M_\odot = 1.989 \times 10^{30}$ kg is one solar mass. For more detail about the assumptions that are used to derive the Jeans mass see e.g. Bisnovatyi-Kogan (2011).

Molecular clouds are mainly composed of molecular hydrogen (H_2) and a small fraction of a rich collection of different molecular species. The low temperature of molecular hydrogen in a molecular cloud makes it essentially invisible to detection devices, as it does not emit radiation that would be

practically detectable from ground-based observatories. The reason for this is that the temperature that is needed to lift an electron to the first energy level for H_2 is 512 K and this is not found in a molecular cloud. Such an H_2 cloud is a radiation sink, and essentially any type of light that has an energy lower than the dissociation energy of H_2 (13.6 eV) is absorbed by the gas. For a thorough discussion of the properties of molecular hydrogen, see Habart et al. (2005).

Carbon monoxide (CO) is a gas that is prominent in molecular clouds and can easily be detected with a radio or sub-mm telescope. CO is a diatomic molecule with an asymmetric structure so, it gives off emission due to molecular rotation in the cm wavelengths and it is massive compared to H_2. A relation exists between CO and H_2: $[H_2/CO] \simeq 10^4 - 10^5$, so that the extent of molecular clouds can be observed through the CO J=1-0 transition. The transition from the J=1-0 energy level of CO contributes to the cooling of the molecular cloud. If it is not possible to do radio probing, molecular clouds can also be detected by means of star counting. If a region of the sky has an unexpected dark patch or a sudden decrease in the number of background stars this may be a sign of a molecular cloud.

Molecular clouds are very absorbent of light due to their dust content so that very little or no light from sources behind or inside the cloud can be detected. Dust grains in diffuse interstellar clouds absorb diffuse light emitted by external stars, re-emitting and scattering the light in the infrared. As the dust grains are in thermal equilibrium and have a typical temperature of 20 K, they emit light in the far infrared and μm parts of the electromagnetic spectrum.

Molecular clouds remain stable for approximately 3×10^7 years before it starts to collapse in under its own weight and becomes very turbulent, according to a theoretical model by Blitz & Shu (1980). If the cloud starts to contract in on itself star formation becomes possible. Once the cloud starts to contract it heats up slightly, and if protostars have formed, they contribute to the internal heating of the cloud, raising temperatures to a range from 50 K to 100 K.

The core of a stable cloud is chemically the richest region of the cloud, can have a particle density of 10^7 cm^{-3}, and can remain stable for up to 10^5 years. Instability of the cloud commences with turbulent motion in the core and then moves outward. For more on the properties, dynamics and detection methods relating to molecular clouds see Kwok (2007), and for the general properties of molecular clouds see e.g. Tielens (2005).

The first type of stars that form are massive OB type stars, close to the outer layers of the molecular cloud because the interior is so turbulent that stable structures cannot form there. When a massive star has formed, it excites the surrounding gas and blows it away. A detailed description of the formation of these stars is given in Lada (1987).

2.3.2 Diffuse interstellar clouds

Diffuse interstellar clouds (DICs) are less dense than molecular clouds, and they do not have definite structures. These DICs are also less opaque than molecular clouds, so that stars behind them can be detected. The clouds are not as optically thick as molecular clouds, but do absorb a fraction of incoming light, so that stable complex molecules cannot be maintained as in molecular clouds, and resulting in a higher presence of diatomic molecules such as H_2, HD, OH and CO. Most of the gas in the galaxy is in diffuse interstellar clouds found in the galactic plane.

2.3.3 HII Regions

An HII region is a luminous nebula of ionized hydrogen which is found around massive stars. These hot stars are of spectral types O and B and have significant ultra-violet emission, making it possible to dissociate H_2 and then ionize hydrogen.

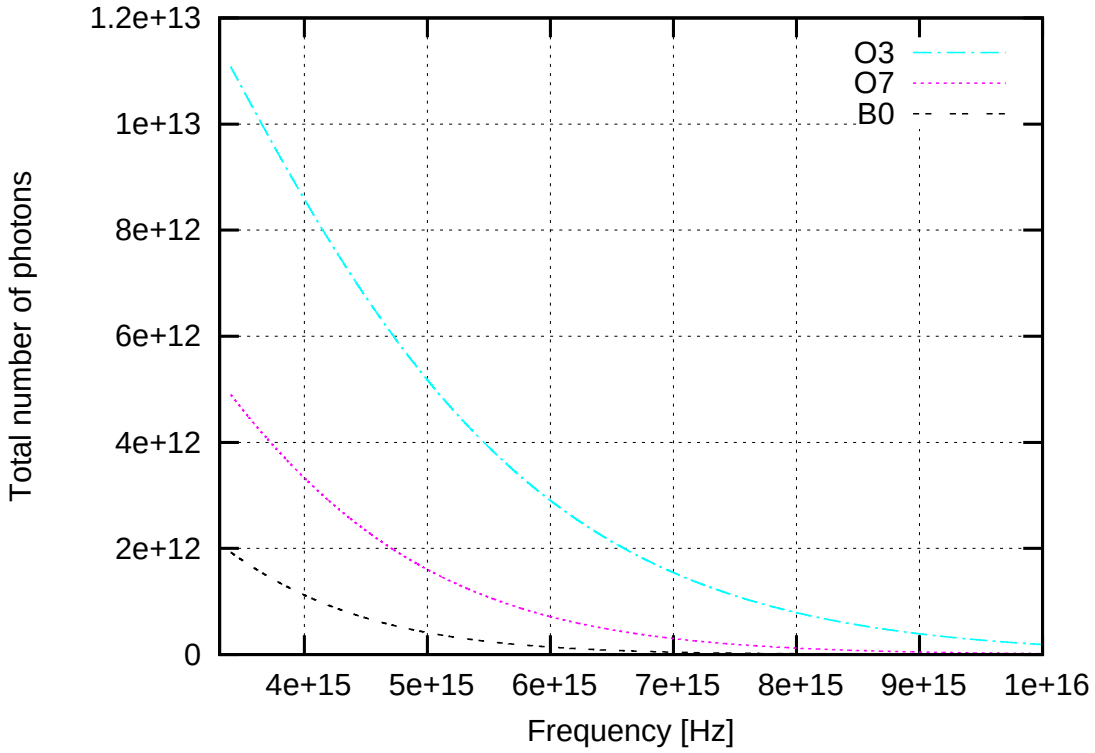

Figure 2.2: The number of ionised particles as a function of frequency for O3, O7 and B0 type stars. The number of ionised particles decreases for stars with a lower surface temperature.

Due to the short lifespans of these massive stars, the molecular clouds in which they are formed are not yet blown away. When they have reached the **m**ain **s**equence (MS) they are still enveloped by gas from the cloud from which they were formed. If a photon has an energy ≥13.6 eV (equivalent frequency of 3.3×10^{15} Hz) and is absorbed by an electron, the electron has enough energy to break free from the atom's potential well. Any excess energy from the photon will serve as kinetic energy for the electron. These massive stars predominantly emit light with an energy lower than the ionization

energy of hydrogen, and the light gets scattered and reddened by the enveloping gas.

To understand the evolution of a young embedded cluster such as RCW 34 in comparison to an open galactic cluster such as NGC 265, one has to understand how the molecular gas is dissociated and blown away by means of photo-ionisation. This can be partly understood by considering the probability that a hydrogen atom will absorb an incident photon based on its cross-section, which is given by Tielens (2005) as

$$\alpha_H(\nu) = \alpha_0 \left(\frac{\nu_T}{\nu}\right)^4 \frac{e^{4\left(1-\frac{tan^{-1}(\varepsilon)}{\varepsilon}\right)}}{1-e^{\frac{-2\pi}{\varepsilon}}} \ , \tag{2.5}$$

with $\alpha_0 = 6.3 \times 10^{-22}$ m^2 the cross-section at the ionisation threshold. Tielens also states that the electrons which break free from their protons will enter the hydrogen cloud and serve as an electron bath. The electrons that break free due to photon absorption collide with those already in the electron bath and reach a Maxwellian velocity distribution. The energy balance between the photon ionisation energy and the kinetic energy of the electrons is

$$\frac{3}{2}kT_H \int_{\nu_H}^{\infty} \mathcal{N}(\nu)\,\alpha_H(\nu)\,\mathrm{d}\nu = \int_{\nu_H}^{\infty} \mathcal{N}(\nu)\,\alpha_H(\nu)\,h(\nu-\nu_H)\,\mathrm{d}\nu \ . \tag{2.6}$$

Emission from the HII region is also due to Bremsstrahlung, which is caused by an excited free electron scattered by the potential well of an ion and emitting some of its kinetic energy as a photon with lower energy. This mechanism causes photons with a wide range of energies to be released, giving the HII region a unique emission continuum.

Free electrons can also contribute to the line emission if they are captured by ions and fall to quantised energy levels. These re-captures increase the strength of the emission lines originating from the ionised gas. When the electron falls to lower energy level it releases a photon with a frequency characteristic to the difference between the energy levels.

If an electron falls from a higher to lower energy level in the gas, it emits a photon for that corresponding wavelength and this results in an increase in the emission line. The rich chemical content of the gas from the molecular cloud gives the emission profile of the HII region a vast collection of emission lines for a vast collection of elements.

The ionised hydrogen has a temperature of roughly 10 000 K, which differs greatly from the average temperature of the molecular cloud (roughly 20 K). This difference causes the ionised gas to have a much higher pressure than the molecular cloud, leading it to expand violently in a “champagne effect” beyond the borders of the molecular cloud. An HII region can be a pointer to high mass stars and active star formation. Due to the immense size of molecular clouds, an HII region is associated with the cloud from which its exciting star has formed. The internal dynamics of a molecular cloud which causes the formation of stars are of such a nature that multiple stars form during the same epoch. A

more in-depth description about the interaction of an exciting star and the luminous nebula surrounding it is given in Lequeux et al. (2004).

This covers the different phases of the ISM where star formation occurs and where young stars are found. The process of star formation is discussed next.

2.4 Star formation

The best way to describe the collapse of a molecular cloud from its cold stable structure to an open cluster, is to construct a theoretical model where the system is treated as a collapse of a uniform gas. The instabilities of an actual molecular cloud due to turbulence, magnetic fields, interaction with other external forces and the gas radiating away energy, cause parts of the cloud to collapse which may be the cause of stellar formation.

Preibisch (2012) gives a detailed discussion of the phases of star formation from an initial molecular cloud to a ZAMS star. Firstly, a dense core forms out of the surrounding matter, becoming optically thick to its own radiation. This can be seen as the start of the star's life. Over the next few thousand years the dense core collapses, and collects more matter from an envelope of surrounding gas which has more mass than the forming core. The envelope absorbs all radiation that emanates from the forming core, and more matter collapsing inwards causes the core to become hotter and hence more luminous. The collapsing envelope does not fall directly onto the forming core, since its angular momentum has to be conserved. The envelope forms a circumstellar disk in a period of less than 100 000 years from which the protostar accretes matter. After the disk has formed, the dust envelope is not as opaque as before, and the core's infrared radiation can propagate outward from the molecular cloud.

The protostar heats the accretion disk so that it emits infrared radiation, which leads to an excess infrared emission for the entire system. The protostar is still obscured by the accretion matter, but emission from the photosphere may be detectable in the near- and far-infrared due to the decrease in matter in the surrounding envelope. This infrared emission from the photosphere makes it possible to detect the protostar, but there is not yet enough light to classify the stellar object.

When the protostar has accreted 90% of its mass, it enters the classical T Tauri phase. It is still surrounded by the optically thick accretion disk, but the photosphere is much less obscured than in the protostellar phase, making it possible to do a spectral/photometric classification. The accretion disk adds to the spectral profile of the star's strong emission lines, specifically the Hα line. The disk also causes excess emission in the near- and mid-infrared to the spectral emission profile of the star, making it an elongated continuum towards the longer wavelengths. A deeper discussion of this will be presented later. A fraction of the accreting matter is collected onto the central star, and a further fraction may condense into planets or other debris, but the majority of the disk is dispersed away by UV- and X-ray emission from the star.

The duration of the classical T Tauri phase has an upper limit of 10^7 years. At the end of this phase, most of the gas in the accretion disk has been dispersed or blown away by high-energy photons. The accretion rate of matter moving from the disk to the star has decreased to an almost static value and the disk may still have some excess emission in the infrared. The equivalent width of emission lines from the accretion disk are very weak relative to their previous values. There are still hydrogen emission lines, but they are much weaker than in the classical T Tauri phase. There are also very young stars without an accretion disk called weak line T Tauri stars.

After the accretion disk has completely dissipated, the spectral profile of the star only shows emission from the photosphere of the star. The mass of the star remains constant and it evolves further towards the hot edge of the main sequence, which is called the **z**ero **a**ge **m**ain **s**equence (ZAMS). As the star approaches the MS, its surface temperature increases. These young stars have strong X-ray emission, absorption lines of Li in their photospheric emission and chromospheric or extreme variable activity. The PMS star may still have a circumstellar disk which is not only composed of gas but also of large dust particles, which are formed by constant collisions and which can lead to the formation of larger structures such as asteroids or planets.

2.4.1 Pre-main sequence stars and accretion disks

In this section a discussion is presented focussing on the PMS phase of young stars. The PMS phase of a star occurs when gravity is the dominating energy source in the star. A PMS star is embedded in the molecular cloud from which it condensed and attracts more matter from its the surroundings which increases the star's mass. During most of the PMS phase, the matter collection continues. The luminosity of the star is not only attributed to nuclear fusion but also to the contraction of the star under its own gravitational field. The energy due to nuclear fusion is provided by means of deuterium burning.

The star contracts at a very slow rate, so it can be treated as if it is in a quasi-static balance between the contracting gravitational force and thermal expansive forces caused by the nuclear reactions in the star's interior. The matter that is collected from the surrounding cloud adds to the star's mass. The higher mass increases the strength of the star's gravitational field, which causes the star's structure to contract and which increases internal pressure. The higher pressure causes the internal temperature to rise, especially that of the core. The PMS phase is the evolutionary stage when a star becomes distinguishable from the surrounding gaseous matter, from the point where hydrogen burning starts in the core as the main power source of luminosity. One tool used to describe the theoretical evolution of a PMS star onto the main sequence, is a Hayashi track first published by Sakashita et al. (1959). There, a model for the evolution of high mass stars was developed where the outer convective layers of the star were simulated.

A Hayashi track starts at the birth line from where the luminosity increases as the star accretes more matter. At the collapse of the star, the luminosity decreases and the surface temperature increases. A Hayashi track gives a realistic fringe between what is possible in a hydrostatic model for

the evolution of the star and what is not.

PMS stars were first classified into groups by Kenyon & Hartmann (1987) in a study of low mass PMS stars in the Taurus-Auriga molecular cloud. The groupings are based on how much matter surrounds the PMS star. This system of classification has become standard in describing the evolutionary stages of young stars: Class 0 is when the core is 20-30 K, basically a dense filament in the molecular cloud. Class I is a protostar that emits in the sub-mm range and usually has an extinction at 1-μm of 10 magnitudes or more. A Class II object is called a classical T Tauri star, which has a hot accretion disk surrounding the star and which contributes to the observed emission profile.

Throughout this stage the **s**pectral **e**mission **d**istribution (SED) for the system changes significantly because of the continued changes to the accretion disk. When matter falls from the disk to the star's surface, the shock gives off a very hot emission, causing the system to have excess infrared, optical and ultraviolet emission. The excess infrared emission easily escapes from the gas surrounding the star and peaks in the J filter. Class III objects are weak-line T Tauri stars, and the accretion disk of these objects has mostly dissipated. A dissipated accretion disk does not emit as much radiation as that of a Class II object, so that the star's emission profile almost resembles that of a MS star. In the evolution between these classes the dominating radiation in the far-infrared progresses from that of a spherical envelope, to that of an accretion disk and ultimately to that of the star. For spectral emission diagrams of the different classes of PMS stars and their interpretation, see Kenyon & Hartmann (1995), Andre et al. (1993) and Andre & Montmerle (1994). An important discussion on the emission in the infrared and sub-mm region by PMS stars is given by Adams et al. (1987).

When an accretion disk has formed in a Class II object, the accretion stabilises to an almost constant rate. Models have been constructed to describe emission from the accretion disk. Previously it was believed that a boundary layer model can describe the excess emission from Class II stars. In the boundary layer model, the rotation of the disk is very slow and decreases closer to the star's surface. Armitage (1995) replaced the boundary layer model with an alternative model, where the magnetosphere of the star keeps the accretion disk at a certain distance from the surface. Matter gets transported to the star's surface via magnetic tubules. This matter hits the star's surface at very high velocities.

A Class II and III PMS will often have an accretion disk with a lower luminosity than that of the central star. In such a case the light absorbed by the accretion disk is the dominant mechanism for heating the disk. If a disk is only heated by irradiation, then it will emit light in a way similar to a black body. If the accretion disk is optically thick and produces more than a quarter of the luminosity from the star it is difficult to distinguish the star and the disk from each other. If the disk is not flat and thin, but extends to a large radial distance, it may absorb much more of the star's radiation. Usually the disk thickness increases away from the central star, and such a disk usually has a flared profile and has an interesting emission profile in the far infrared. For the mathematics involved in the

illumination of the accretion disk, see Hartman (1998).

2.5 T Tauri stars

2.5.1 Introduction

Joy (1945) was the first to mention a T Tauri star in the literature and defined it as a new type of variable star. The abbreviation is short for the third type of variable star that was discovered in the Taurus nebula. T Tauri stars belong to a class of PMS stars with a mass range between 0.5 $M_\odot$ and 2 $M_\odot$.

A thorough description for the properties of T Tauri stars follows. It is a summary of sections in Hartman (1998). The description covers the general properties of T Tauri star. More details of the two types of a T Tauri classifications follow, along with the spectroscopic particulars of T Tauri stars.

2.5.2 General properties of T Tauri stars

T Tauri stars exhibit excess ultraviolet, optical and infrared emission. They also have variable radio and X-ray emission which is much stronger than that seen in main-sequence stars. The most prominent feature seen in the spectrum of every T Tauri star is an Hα emission line. Some very young T Tauri stars also exhibit a strong Li absorption line.

T Tauri stars have two classes into which they can be divided: **c**lassical **T T**auri stars (CTTs) and **w**eak line **T T**auri stars (WTTs). The distinction is made on the basis of the equivalent line width of the Hα emission line. A WTT will have an Hα-emission line with an equivalent width of 10Å or narrower. A CTT has an accretion disk that guides matter to the central star, whereas for a WTT this will not be seen. The emission mechanism for the Hα line is different for the two classes. Each class is characterised by a very strong magnetic field and vast amounts of matter close to the star's surface.

Lynden-Bell (1974) first mentioned that the excess emission seen in T Tauri stars could originate from an accretion disk. It was also suggested that the accretion disk may be very dusty, which may account for the excess emission in CTTs. WTTs show coronal emission similar to the sun, but much stronger. Roughly 60 percent of T Tauri stars that are younger than $3{\times}10^6$ years have excess NIR emission, which may be attributed to an accretion disk.

Some T Tauri stars of both classes have a variation in brightness. The average period for the variation can have a value between one and twelve days. Such variations can occur due to large star spots which are similar to sunspots but appear much bigger due to circumstellar matter moving between the star and observer. Irregular variations can also occur due to flaring. These are usually of the order of 3 magnitudes.

On a luminosity-temperature diagram, a T Tauri star will lie above the main sequence. It will display a luminosity higher than a star of the same mass on the main sequence and has a lower surface temperature. This is common for PMS stars. The T Tauri will be on a Hayashi track for its spectral class, somewhere between the birth line and the 10^7 year line. This means that the colours of the star will be bluer than what one would expect from a star in the same spectral class in the main-sequence.

The main fuel source for a T Tauri's luminosity is gravitational collapse, as it is not yet at a stage where hydrogen burning can be the main fuel source. The star first depletes its deuterium supply through deuterium-burning, which serves as an extra source of luminosity. For more on the characteristics and observational history on T Tauri stars, see Kogure & Leung (2007). The rest of the chapter consists of sections that describe the properties of CCTs, WTTs, a third class of T Tauri stars and groupings of T Tauri stars.

2.5.3 Classical T Tauri stars

The classical T Tauri was discovered and first defined by Joy (1945). As a star which has excess emission and is surrounded by an invariable accretion disk. The accretion disk is the source of the excess emission and of emission lines not seen in naked stars. A description of the geometry and the mechanics of the accretion disk is given followed by a brief discussion in the the driving mechanism behind the emission lines.

2.5.3.1 Geometry of the accretion disk

In section 2.4.1 it was stated that the boundary layer model was replaced by an accretion disk model. According to the accretion disk model a CTT has a very strong magnetic field which influences the geometry of the accretion disk.

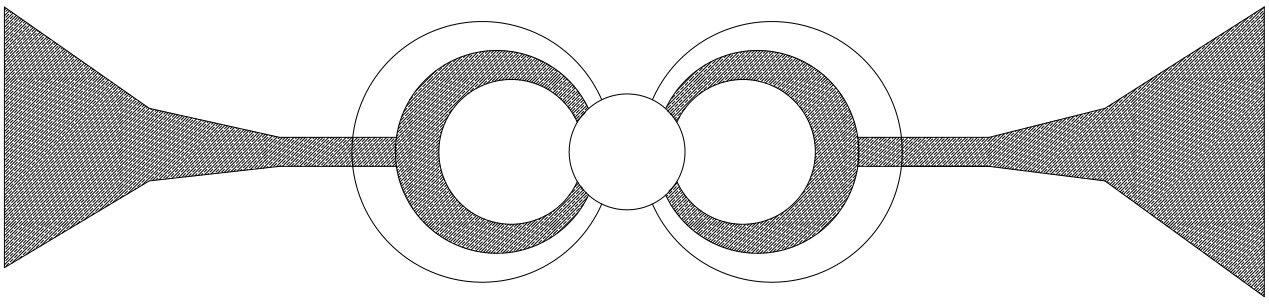

Figure 2.3: A reproduction of a schematic drawing from Hartman (1998) representing the accretion disk around a classical T Tauri star.

In Fig 2.3 a cross section of the accretion disk around a CTT is shown. The disk starts as a widely separated body starting from the dust envelope far away from the star. It is the dust in this wide part of the accretion disk furthest from the star that is responsible for excess infrared emission. It is also

the most prominent mechanism responsible for the scattering of light emitted from the star.

The matter in the disk closer to the star has a higher angular momentum and the structure narrows accordingly. At a critical distance from the star the magnetosphere brakes the structure of the accretion disk. The region from the braking point towards the star's surface is clear of matter forming part of the disk. Matter moves in magnetic tubules from the braking distance to the star's surface. The field's influence on the matter from the accretion disk is of such a nature that it falls onto the protostar at high latitudes. The meeting point between the outer circles with the stellar surface represents the accretion shocks as shown in Fig 2.3. Matter in these tubules move at free-fall velocities and generate shocks on the star's surface, causing the excess optical and ultraviolet emission. In the following section a more detailed description is given about these shocks and how they cause the excess emission.

2.5.3.2 Excess emission from the accretion disk

The accretion disk is the main source of excess ultraviolet, optical and infrared emission. To explain the mechanisms which cause the excess emission, an example from Hartman (1998) of an average T Tauri star is used. It has a mass of 0.5 $M_{\odot}$, radius of 2 $R_{\odot}$ and matter falling in at a velocity of 200-300 km/s. The matter moving in the magnetic tubules will hit the surface with a significant shock and can be heated to a temperature of T$\approx 10^6$ K. This hot gas is not optically thick and will give off immense amounts of radiation towards and away from the star. Emission that is projected away from the star will have to propagate through the embedding dust envelope which is optically thick. The observed spectrum emitted by the hot gas will be substantially altered.

Lynden-Bell (1974) postulate that the accretion disk may outshine the central star. However, T Tauri stars are brighter than their accretion disks, and the disks are mainly heated by irradiation rather than viscous heating. In very young PMS stars the accretion disk may outshine the central star during outbursts.

This explains the excess optical and ultraviolet emission seen in T Tauri stars. Excess infrared emission, on the other hand, emanates from heated dust in the accretion disk. The infrared excess peaks in the J-filter and dominates all the excess emission seen from such a star-disk system. The infrared emission originates further away from the central star and the dust is optically thin for infrared and longer wavelength emission. The dust heated by irradiation provides the excess infrared radiation and will settle at the central band of the disk. The structure of the dust particles will determine at what rate they will settle in the inner part of the disk and for how long they will be suspended.

The continuum is much flatter than one would expect and is caused by thermal emission from the dust in the accretion disk. Currently the reason for the flat continuum is not yet fully understood. A possible reason is that the accretion rate is constant for different radial distances. The temperature distribution of matter in the accretion disk is not yet understood.

A model by Garcia et al. (2001) assumes that the disk is not just heated by irradiation but also by ambi-polar diffusion which can describe the flat SED. Ambi-polar diffusion occurs in a weakly ionised plasma, where the ions and electrons jointly diffuse against a background of neutral particles. The dominant heating and cooling mechanism in the disk is respectively ambi-polar heating and adiabatic expansion. The model also explains the origin of forbidden lines that are observed in T Tauri spectra. These lines are formed in cold jets that originate from the stellar surface and are only powered by a Lorentz force.

By knowing the correct emission from the photosphere of the star, the correct extinction to the star can be calculated. To correctly calculate the excess emission contributed by the accretion disk, the unobserved emission also has to be taken into account.

2.5.3.3 Spectroscopic properties of CTTs

The source of the various emission lines seen in the SED of T Tauri stars is believed to be the matter moving from accretion tubules onto the star's surface. Emission lines observed in the spectral profile of a T Tauri star may be very wide for CTTs, depending on how much matter is transported onto the star.

The most common lines are the H and K lines of Ca II, Hα and Fe I, but many others are seen in the SEDs. The most prominent and strongest of these lines is the Hα emission line. An important feature of a young T Tauri star is the presence of a strong Lithium absorption line at a wavelength of 6707 Å. Lithium is not found in the spectra of MS stars because it is burnt up very early in a star's lifetime.

Fig 2.4 shows low resolution spectral profiles for eight CTTs in the Taurus-Auriga star forming region. In each profile, the hot excess emission is obvious. This is caused by the dissipation of the energy from matter falling onto the stellar surface. The matter that is transported in the accretion tubules moves at a very high velocity onto the slowly rotating stellar surface, causing the hot emission shown in the Balmer series.

To determine the mass/spectral type of the star is difficult because the optical emission from the accretion matter will make the light from the entire system bluer than the photosphere's emission alone. This type of system is almost always embedded in the molecular cloud it formed out of, which will add extinction to the intrinsic colours of the system. To calculate the extinction to the star the intrinsic colours of a standard star of the same spectral type will have to be known. The excess emission by the hot infalling matter is significant for some cases and will have to be accounted for, otherwise the extinction may be underestimated. The estimation of the excess emission is not an easy task as the range of the temperatures for the infalling matter is not known.

If one knows the spectral type of the star, then the relative strengths of the standard star can be

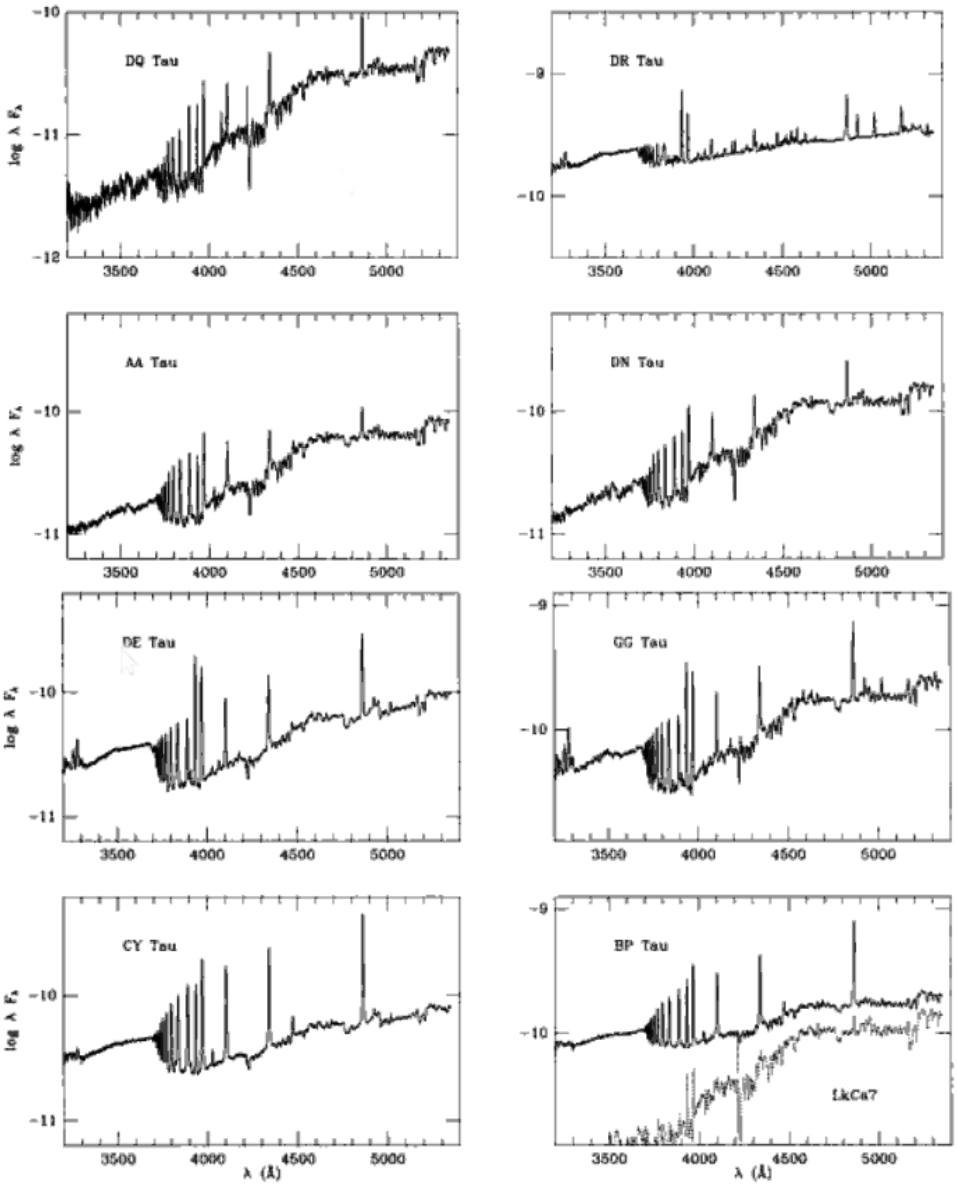

Figure 2.4: Eight different spectral profiles of T Tauri stars as shown in Fig 6.6 of Hartman (1998).

used to separate the emission from the photosphere of the observed star and the hot emission from the infalling matter. Hot emission from the in falling matter will add to the light emitted from the absorption lines in the photosphere - it will seem that the absorption lines are not as strong as they actually are.

2.5.4 Weak line T Tauri stars

WTTs are stars that exhibit an Hα emission line with an equivalent width of 10 Å and less. The Hα emission from WTTs is caused by chromospheric emission due to a thick layer of matter close to the stellar surface. A WTT exhibits the same type of coronal emission and magnetic field as the Sun. By

understanding the emission mechanism for the Hα-line in WTTs it is possible to understand the cause of the Hα emission line in CTTs. The lack of an accretion disk accociated with a WTT can be due to an instability in the accretion disk due to the presence of a binary member of the host star.

The velocity that is observed in the Hα-emission line for a WTT is generally lower than that of a CTT, having an average value of 100 km/s. WTTs do not collect matter from accretion disks in the same way as CTTs do. The lack of an accretion disk implies that a WTT will not exhibit excess emission in the infrared as a CTT would. This also implies that a WTT does not have the hot emission from matter transferred onto the stellar surface as in the case of CTT. See Duvert et al. (2000) for a discussion on the circumstellar matter around WTTs.

It may be difficult to distinguish between CTTs and WTTs on the basis of equivalent widths of Hα lines only. A few fringe cases have led to the rethinking of the 10 Å Hα-line definition, which was initially based on M class stars. The amount of infalling matter that creates a strong or wide emission line for an M type star may create a much weaker emission line for an F or G type star, and it may even show an absorption effect.

A very important point to be made is that the temperature of the photosphere of the star has a large effect on the strength of the Hα lines. For a deeper discussion of the theoretical basis of the argument that the 10 Å distinction between CTTS and WTTS is not good, see Cram & Mullan (1985).

2.5.5 The third class of T Tauri star

A sub-class of T Tauris relates to stars with a flat continuum. An example of such a star is HL Tauri, studied by Beckwith et al. (1989). The disk will need a constant temperature power-law throughout the structure, which can only be attained by means of irradiation if the disk flares immensely for a vast range of distances from the star.

The flat profile of the SED will start in the optical and extend into the infrared or even longer wavelengths. In a few cases the optical light observed from such sources will be scattered by an infalling dust envelope. The dust envelope and the NIR part of the SED matches with those characteristic to protostellar sources in the Taurus star forming region, and what is expected from protostellar sources.

The inclination angle for the disk of such an enclosed star may result in it being classified as a Class I PMS star instead of a T Tauri if not properly studied. This can occur if the dust envelope is so dense in the direction of the observer that the optical light is completely absorbed, so that mm and longer wavelength emission is seen. The dust that surrounds the star acts as a blanket for the escaping radiation and is a second heating source for the disk. This scenario is not a general one and may be the case of a matured protostar still surrounded by a dust envelope, but with a T Tauri star at the centre.

Another scenario is when a T Tauri has a closely situated protostellar companion with a heated dust envelope. This adds the excess emission to the star's SED, creating a flat continuum. The dust envelope has such vast dimensions that it may envelope the accompanying star. T Tauri itself is such a case, as it has a flat SED which is the result of a closely situated companion.

2.5.6 Groups of T Tauri stars

T Tauri stars are not found alone but always in groups closely located or embedded in molecular clouds. When a massive OB star association forms, it excites and blows away the gas surrounding it very quickly. This disturbance of the molecular cloud causes the low-mass stars that form from the same cloud to expand away from the association.

These low mass young stars are called a **T association** or a collection of T Tauri stars. The distribution of young stars indicates the initial morphology of the parent cloud. The young age of the T Tauri stars does not allow the expanding association to move far from this initial morphology. T associations come in a variety of forms, the closest one to us being TW Hydrae a small association only 50 pc away. A much more active T association is NGC 1333 in the Perseus cloud, complex close to the Vela cloud complex.

A T association will contain both visible and obscured objects, which is indicative of the gas of the initial cloud not yet having been blown away by the young stellar objects (YSOs). The proper motions of both the CTTs and the WTTs are very similar to the proper motion of the gas cloud.

Associations in the region close to our solar system do not reveal a high concentration of embedded clusters. The local T associations have between five and twenty members. An association that has classical and weak line T Tauri stars is an indication of active star formation. For a more in-depth discussion on the local T associations and details of each see Palla & Stahler (2005).

A theoretical basis and discription about the tools that will be used to study RCW 34 and search for T Tauri stars will be given next. It will start with photometry, which is the direct imaging of a chosen field of view, and then the tools used to analyse the photometric data. The photometric section will include sections on how interstellar matter interacts with the light insedent from stars. This will be followed by a short section on spectroscopy.

2.6 Photometry

2.6.1 The magnitude scale, flux and luminosity

The magnitude scale was first introduced by the Greek astronomer Hipparchus when he compiled the first catalogue of 850 stars. He catalogued each stellar position and assigned an apparent magnitude

according to the brightness. The brightest of these stars were given a magnitude of 1 and the dimmest a magnitude of 6, so that the dimmer a star appears, the higher its magnitude. This arcane system has become the standard tool for measuring the "brightness" of a star.

In the nineteenth century it was discovered that the human eye recognises the difference in the brightness of different objects on a logarithmic scale. The magnitude scale was thus adapted to fit this logarithmic scale, whereby a magnitude difference of five indicates that the object with the higher magnitude is one hundred times fainter than the brighter one. A magnitude difference of 1 would therefore indicate a ratio of brightness differences of $100^{1/5} \simeq 2.512$. Using this definition of magnitude one can calculate the flux ratio between two stars as

$$\frac{F_1}{F_2} = 100^{(m_1 - m_2)/5} \ , \tag{2.7}$$

with m_1 and m_2 the different magnitudes. Taking the base 10 logarithm of each side gives

$$m_1 - m_2 = -2.5 \times \log_{10}\left(\frac{F_1}{F_2}\right) \ . \tag{2.8}$$

A star's brightness is measured in terms of its **radiant flux**. This is the total energy emitted by the star at all wavelengths that propagates perpendicular across a specific area per time unit - the number of Joules is received by a detector per second. This flux depends on two factors: the luminosity of the star, and the distance between the observer and the star. The relation between the flux (F [W/m^2]), luminosity (L [W]) and the distance (r) is

$$F = \frac{L}{4\pi r^2} \ . \tag{2.9}$$

This relation states that the flux decreases proportionally the square of the distance between the source and the observer. If one measures the magnitude of a star by plainly measuring the flux and compensating for atmospheric extinction, one is measuring the **apparent magnitude**.

Using the apparent magnitude of a star, one can calculate the **absolute magnitude**. The absolute magnitude is the magnitude a star would have if it was at a distance of 10 pc. The absolute magnitude of a star can be calculated by using the **distance modulus**, which is the difference in magnitude of a star at its normal distance and its magnitude at a distance of 10 pc. If one substitutes the distance in equation (2.9) and the flux from the star at 10 pc, the distance modulus is calculated in terms of the ratio of the observed flux to that of what it should be at 10 pc

$$100^{(m-M)/5} = \frac{F_{10}}{F} = \left(\frac{d}{10 \text{ pc}}\right) \tag{2.10}$$

or

$$m - M = 5log_{10}(d) - 5 = 5\log_{10}\left(\frac{d}{10 \text{ pc}}\right) \ , \tag{2.11}$$

where m is the apparent magnitude, M is the absolute magnitude, F_{10} the flux of the star at a distance

of 10 pc and F the apparent flux of the star at its observed distance d. The history, and details of the magnitude scale are thoroughly discussed by Carroll & Ostlie (2007).

2.6.2 The CCD and filter systems

2.6.2.1 CCD

In modern-day astronomy, a CCD (Charged Coupled Device) is the standard detector used for astronomical observations. It was invented by Boyle and Smith in 1971 at Bell laboratories. For more on the developmental history of the CCD see Chromey (2010). A CCD is constructed from the semiconductor element silicon in a pixel based array of MOS capacitors that stores photo-electrons in a potential well. If the array is exposed to a light source it accumulates photo-electrons in the potential wells,the number of photons accumulated is proportional to the time the CCD is exposed to light.

The intensity of the photon flux at a depth z in a semiconductor such as a CCD is

$$I(z) = I(0)\, e^{-\alpha z} \,, \tag{2.12}$$

where α is the absorption coefficient and $I(0)$ is the intensity at the surface. The absorption coefficient is proportional to the temperature, so if the temperature decreases a photon can penetrate deeper into the material before it is absorbed. If a photon is absorbed into a semiconductor such as the silicon chip the photo-electron bound in the valence band has enough energy to move into the conduction band.

The crystalline structure in a CCD chip is arranged in such a way that the distribution of light on the chip is outlined by the number of conductive electrons in a pixel. The number of electrons in each pixel is read out, and a digital image is constructed.

2.6.2.2 Filter systems

A standard photometric system of filters for the optical lightband was designed and described in a series of papers by Johnson (1952). Johnson introduced the UBV filters, which have respective peak efficiencies at 3500 Å, 4300 Å and 5550 Å. Bessell & Brett (1988) give a comparison between two different VRI filter systems: The Kron system, which is commonly used in the Southern hemisphere and the Cousins system which is commonly used in the Northern hemisphere see Bessell (1979) and Bessell (1986). Internationally the Johnson-Cousins filter system ($UBV(RI)_{(c)}$) is accepted as standard. The transformation equations from the Kron to the Cousins systems are given by Bessell & Weis (1987) as

$$\begin{aligned}
(V-R)_c &= 0.113 + 1.0609\,(V-R)_{KR} - 0.3303\,(V-R)^2_{KR} + 0.0851\,(V-R)^3_{KR} \,, \\
(R-I)_c &= 0.102 + 0.9166\,(R-I)_{KR} + 0.4230\,(R-I)^2_{KR} - 0.16647\,(R-I)^3_{KR} \,, \\
(V-I)_c &= 0.227 + 0.9567\,(V-I)_{KR} + 0.0128\,(V-I)^2_{KR} - 0.00530\,(v-I)^3_{KR} \,.
\end{aligned} \tag{2.13}$$

By using the relation between the radiative flux and the magnitude in equation 2.8, an expression can be constructed for the magnitude M_λ that is measured in a filter λ, neglecting the effects caused

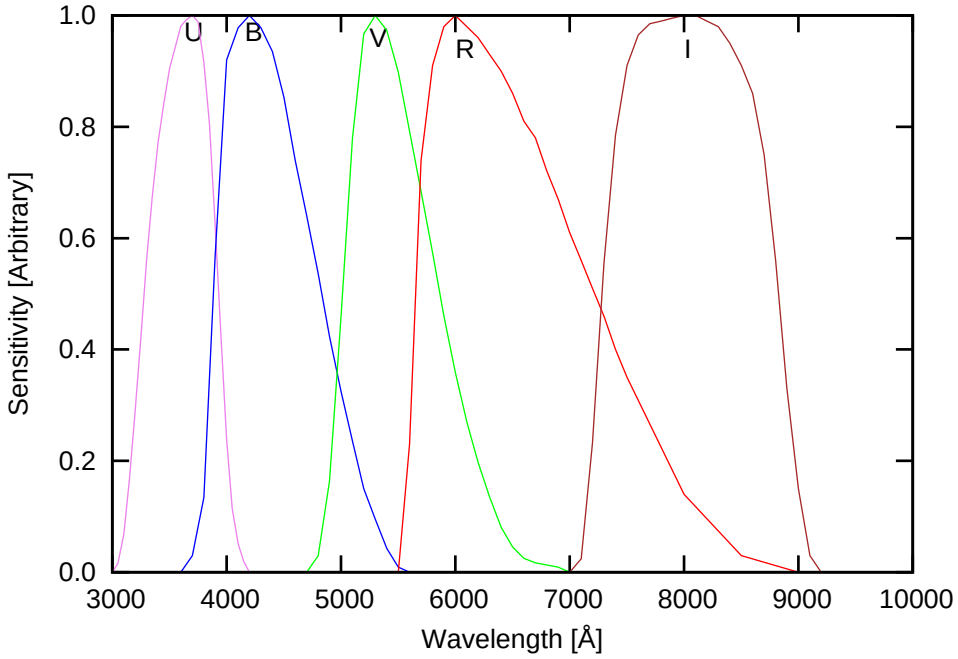

Figure 2.5: This is a reproduction of Fig 1 in Bessell (2005), on the x-axis is the wavelength in Å and on the y-axis is an arbitrary unit representing sensitivity. The five Johnson filters are plotted for the amount of light that each lets through against the wavelength.

by the Earth's atmosphere.

A **sensitivity function** is defined as the fraction of light in the filter λ detected from the star. The sensitivity function is dependent on the telescope's diameter, the effectivity of the CCD and numerous other factors. The range of the electromagnetic spectrum allowed to pass each filter is shown in Fig 2.5. The magnitude M_λ is given by

$$M_\lambda = -2.5 \log_{10}\left(\int_0^\infty F_\lambda S_\lambda d\lambda\right) + C_\lambda \ , \tag{2.14}$$

with C_λ an arbitrary calibration constant so that the filter λ would have a value of zero for the star Vega, F_λ the flux of the light in the filter λ, and S_λ the sensitivity of the CCD to the light that is allowed through for filter λ.

2.6.2.3 Signal-to-noise

The quality of an image is measured by the signal-to-noise ratio $\left(\frac{S}{N}\right)$. The signal (S) refers to the photons that originated from the desired source and the noise (N) refers to random photons that originated from any unknown source along with statistical noise.

Chromey (2010) gives an example of how a telescope with an aperture D observes a star that emits a flux f_λ for a time duration of t. The emitting flux f_λ is not the intrinsic flux of the star but is subject to atmospheric and interstellar extinction and to the distance to the star. The number of photons that

will be detected by the telescope is

$$S = \text{signal} = \frac{\pi D}{4}\frac{\lambda}{hc} f_\lambda t Q \ , \tag{2.15}$$

where Q is a quantum effectivity factor dependent on how much light is let through by the filter λ and the efficiency of the detector for that filter, and where $\frac{\lambda}{hc}$ converts the energy units to a number of photons. The star will be *detectable* if its signal is of the same magnitude as its uncertainty. The uncertainty can be understood using the combined signal and background of a faint star. The *background* is the measurement of the sky, which is a composition of diffuse photons that can come from any source, i.e.

$$\text{measurement} = S + B \ . \tag{2.16}$$

The signal is calculated by subtracting the background in the observed stellar field from the total measurement. If the star in the field has an angular diameter of Θ and the sky has a brightness of b_λ then the background is given by

$$B = \text{background} = \frac{\pi D^2}{4}\frac{\lambda}{hc}\frac{\pi\Theta^2}{4} b_\lambda t Q \ . \tag{2.17}$$

A faint star's contribution to the measurement can be ignored. However, there remains uncertainty as to what other unknown sources are included in the background of an image, and if a faint star is included in a measurement, then it can be regarded as one of these unknown sources. The uncertainty can be defined as the *noise*, which is a combination of the uncertainty of where the photons originated and statistical noise. For the number of photons considered, one uses Poisson statistics where the noise is calculated as

$$N = \text{noise} = \sigma(S) = [(S + B) + B]^{\frac{1}{2}} \simeq \sqrt{2B} = \frac{\pi D\Theta}{4}\left(\frac{2\lambda b_\lambda t Q}{hc}\right)^{\frac{1}{2}} \ . \tag{2.18}$$

Using equations 2.15 and 2.18 the **signal-to-noise** ratio is

$$\frac{S}{N} = \left(\frac{\lambda Q}{hc}\frac{t}{b_\lambda}\right)^{\frac{1}{2}} \frac{D}{\Theta} f_\lambda \ . \tag{2.19}$$

The relation $\frac{S}{N} \propto \sqrt{t}$ is a limiting factor if one wants to get a better quality image and see fainter objects; to double the $\frac{S}{N}$ the exposure time has to increased fourfold.

When doing direct imaging one must be careful not to extend the exposure time of a single image because the CCD can become saturated if the number of photo-electrons in any pixel exceeds the capacity of the pixel. Another phenomenon that can occur when doing long exposures of direct imaging is the effects of cosmic rays, which can imprint on the CCD and create a very high reading on one or two pixels, depending on the angle of incidence of the cosmic ray relative to the CCD.

2.6.2.4 Intrinsic colours and temperature

In a photometric system, a **colour** is defined as the difference of two magnitudes in different filters for a star. The $U-B$ and $B-V$ colours each have a value of zero for an $A0V$ type star, and they are used to calibrate the other colours in the Johnson-Cousins system. The standard star on which the colour-system is based is Vega.(for more on this system see Chromey (2010)). The $UBVRI$ filter system is used as a crude spectral system due to the filters being sensitive to specific bands of the optical region. The colours are sensitive to the temperature of a star that emits light. They can be used to determine the surface temperature of a star and identify the spectral type of the star. This is possible because each spectral type has a set of **intrinsic colours** which allows for classification on a colour-colour diagram, for example $V-R$ against $R-I$.

The colour indices of a star are indicate to the temperature of the star, for example if the $U-B$ colour has a smaller value than the $B-V$, the star has a higher flux in the blue part (≈ 3000 Å) than in the red part (≈ 7000 Å) of the spectrum and this indicates a warm star (O or B spectral type). A cooler star (K spectral type) will have a higher $B-V$ value than $U-B$. A warm star's Planck spectrum peaks in the blue part of the spectrum and that of a cool star in the red part.

An example from Carroll & Ostlie (2007) shows a star which has a surface temperature of 42 000 K and colours of $U-V=-1.19$ and $B-V=-0.33$. Using Wein's displacment law $\lambda_{max}T = 2.898\times10^{-3}$ m.K one can calculate the maximum wavelength as

$$\lambda_{max} = \frac{2.898\times10^{-3}\ \text{m.K}}{42000\ \text{K}} = 69\ \text{nm}\ . \tag{2.20}$$

This lies far in the ultraviolet part of the spectrum, so the $U-B$ colour will have the maximum value in the continuum emission and decrease towards longer wavelengths.

2.6.3 Interstellar extinction

Interstellar space is close to a perfect vacuum, where on average the ISM in interstellar space has a density number of 50 particles.cm^{-3}. However, due to the vast distances between stars, the amount of gas through which the light should propagate before being observed is substantial. In this way light gets extinct by the ISM. For a list of all of the phases of the ISM, see Table 1.1 in Tielens (2005).

The extinction of light is wavelength-dependent, so that ultraviolet light is much more easily absorbed by the ISM than infrared light. Extinction associated with a specific filter is measured as a factor for the visual filter. The extinction for each Johnson-Cousins filter as a factor of the visual extinction is shown in Fig 2.6.

The absolute magnitude of a star in a filter λ is given by

$$m(\lambda) = M(\lambda) - 5\log_{10}\left(\frac{d}{10}\right) - A_\lambda\ , \tag{2.21}$$

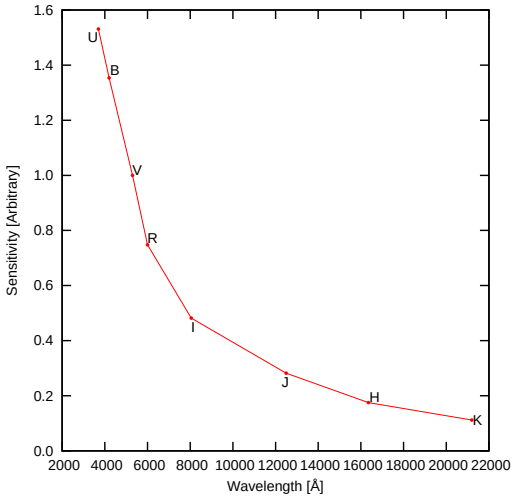

Figure 2.6: The extinction for visual filters as a factor of the visual extinction A_v. The optical filters are the same as those shown in Fig 2.5. Extinction is wavelength dependent and photons in the ultra-violet are much better absorbed by interstellar gas than infrared photons.

where m is the absolute magnitude, M the apparent magnitude and A_λ the extinction by interstellar dust for the given wavelength λ.

The colour excess that is added by interstellar reddening between two wavelengths λ_1 and λ_2 is

$$E(\lambda_1 - \lambda_2) = A_{\lambda_1} - A_{\lambda_2} \ . \tag{2.22}$$

Generally the reddening is less for magnitudes of longer wavelengths and one can compare the ratio of the excess between two colours for a source. The excess in the $B-V$ colour is expressed relative to other colour excesses as

$$\frac{E(\lambda - V)}{E(B-V)} = \frac{A_\lambda - A_V}{A_B - A_V} \ . \tag{2.23}$$

Rieke & Lebofsky (1985) determined the relation between extinction in different filters. The absorption of short wavelength photons is much more prominent than that of long wavelength photons, and the extinctions are normalised to the visual extinction A_V. The excess colours were also normalised to the excess in the $B-V$ colours, and the relations are given in Table **??**.

2.7 Spectroscopy

Atoms or ions can emit or absorb radiation in the form of photons by the transition of electrons between energy levels. Radiation is absorbed when an electron "jumps" from a lower to higher energy level. Likewise, radiation is emitted when an electron "falls" from a higher to a lower energy level. These quantised energy levels are unique to each chemical element and are used to identify these elements in a star's emission profile. There are three ways in which an electron can change in energy levels; it can spontaneously emit radiation, the atom can emit radiation if it is exposed to radiation with an energy

λ	$\frac{E(\lambda-V)}{E(B-V)} = \frac{A_\lambda - A_V}{A_B - A_V}$	$\frac{A_\lambda}{A_V}$
U	1.64	1.531
B	1.00	1.324
V	0.00	1.000
R	-0.78	0.748
I	-1.60	0.482
J	-2.22±0.02	0.282
H	-2.55±0.03	0.175
K	-2.744±0.002	0.112

Table 2.1: The interstellar extinction law as given in Table 3 of Rieke & Lebofsky (1985)

equivalent to the transition energy (i.e. stimulated emission) and then an atom can partially absorb a photon if exposed to radiation with various wavelengths and jump to a higher energy level.

During spontaneous emission the number of photons that are emitted with a frequency $\nu_{nn'}$ due to the transition of electrons moving from level n to n' can be expressed as $A_{nn'}N_n$. Here $A_{nn'}$ is the Einstein coefficient for the probability that a transition from level n to n' will occur per unit volume per second, and N_n is the number of electrons in level n. For stimulated emission, the number of transitions from level n to n' is proportional to the intensity of the radiation field incident on the atoms $J_{nn'}$. The number of transitions that occur due to stimulated emission per unit volume per unit time is $B_{nn'}N_nJ_{nn'}$ with $B_{nn'}$ the Einstein coefficient for electrons that go from level n to n' through stimulated emission. If a radiation field with intensity $J_{nn''}$ is incident on matter, the photons with a frequency $\nu_{nn''}$ will be absorbed and move from level n to n''. The number of photons that are removed from the radiation field with frequency $\nu_{nn''}$ is $B_{nn''}N_nJ_{nn''}$. For more on Einstein coefficients and radiative transfers see Tielens (2005).

Spectroscopic images are different from photometric images in the way that light is distributed on the CCD chip. In the case of photometry, light is directly displaced through the telescope, and a filter and then onto the CCD chip. For long-slit spectroscopic images, the light moves through the telescope and is dispersed by a slit in the same way that a prism disperses light. After dispersion, the light is collimated by a dispersion grating with fixed resolutions of 1 Å, 2 Å, 5Å ... etc. The angle of the grating determines which part of the electromagnetic spectrum is viewed and the resolution of the grating determines the detailed analysis. From the grating, the light is reflected onto a CCD chip making it possible to distinguish absorption and emission lines. For more details on the type of hardware that can be used for spectroscopy see Chromey (2010).

Absorption lines are formed if radiation is released due to thermonuclear reactions in the core and moves through the outer layers of the star. The outer layers are cooler than the core and are heated by the absorption of the energy emanating from the core. If energy is absorbed by an electron in a certain energy state of an element, the total flux of energy moving through the star, which eventually

emanates from the photosphere, will have a lower reading for the frequency ν of the absorbed radiation in the continuum than what is expected for a black body. The electron uses energy absorbed from radiation (of frequency ν) to break free from its specific energy level in the potential well, and move to a higher energy level or break free from the atom. Due to the chemical make up of stars the most prominent element is Hydrogen, and which has the strongest absorption.

According to Kogure & Leung (2007) emission lines can occur due to three causes: (1) stellar envelopes that expand due to strong stellar wind, rotating disks, accretion disks, chromosphere-corona structure and pulsating atmospheres; (2) stellar activity which may be in the form of flare outbursts or dark and bright spots in the photosphere; and (3) binary interactions where mass exchange occurs between stars, e.g. cataclysmic variables.

This chapter dealt with many properties of T Tauri stars, not all of which are applicable to this project. It was nevertheless deemed appropriate to provide an extensive background to these subjects addressed in this study. The following chapter contains short complementary sections of theory that are directly relevant to the reduction process applied to the data gathered by means of telescopic observations.